Arch. Bas. App. Med.12 (2024):10-18
www.archivesbamui.com
www.ojshostng.com/index.php/abam

Research Article

Dose dependent ventricular enlargement, neurodegeneration and mortality rates in kaolin-induced hydrocephalus in adult mice

Femi-Akinlosotu O.[1], Olopade, F.[1], Abe, B.[1] and *Shokunbi M.[1,2]

[1] *Department of Anatomy, College of Medicine, University of Ibadan. Nigeria.*
[2] *Division of Neurological Surgery, Department of Surgery, University of Ibadan. Nigeria*

Accepted: January 24, 2024

Abstract

Intra-cisternal injection of kaolin is the most common method of experimentally inducing hydrocephalus. A reduction in kaolin dosage has been reported to reduce the mortality rate. Thus, the mortality rate and degree of ventricular enlargement in adult male mice with the use of different concentrations of kaolin suspension to induce hydrocephalus and observed the morphological changes in pyramidal neurons of layer V of the sensorimotor cortex and hippocampus were compared.

Hydrocephalus was induced intracisternally in adult male mice subdivided into 5 groups (n=27) using 0.02mL of 50, 100, 150, 200 and 250 mg/mL of kaolin respectively while controls (n=15) received sham injection. Mice were weighed biweekly for 4 weeks. Harvested brains were processed for Cresyl violet and NeuN Immunostaining to assess neuronal damage. Data were analyzed using GraphPad Prism 8 and ImageJ software. The hydrocephalic rates of 50, 100, 150, 200 and 250 mg/mL groups were 40.0%, 58.8%, 78.6%, 88.9% and 94.4% respectively while their mortality rates were 21.1%, 22.7%, 26.3%, 28.0% and 30.8% respectively. The mortality rate and frequency of hydrocephalus in 250 mg/mL group were significantly higher than 50 and 100 mg/L groups ($p<0.0001$), while there was no significant difference between the ventricular diameter in 250 mg/mL group and others ($p=0.0002$). Pyknotic pyramidal neurons of the sensorimotor cortex of mice induced with 250 mg/mL group of kaolin concentration were significantly more numerous than the control ($p<0.05$). The pyknotic index (PI) of the dentate gyrus in the 250 mg/mL group was significantly higher than the control. NeuN immunohistochemistry of Layer V of hydrocephalic brains demonstrated decreased staining intensity and fewer NeuN-positive cells compared to controls. The findings from this study suggest that for the induction of hydrocephalus in adult mice, the use of 150 mg/mL and 250 mg/mL concentrations are suitable for long and short-term studies respectively.

Key Words: kaolin, hydrocephalus, pyramidal neurons, pyknotic index, sensorimotor cortex

INTRODUCTION

Hydrocephalus is a common neurological disease characterized by abnormalities in secretion, circulation, and or absorption of cerebrospinal fluid (CSF) leading to an increase in intracranial pressure (Del Bigio, 2010; Bothwell, Janigro, & Patabendige, 2019; Azzam, Yehia, Abd El-Bary, & El-Sharkawy, 2023), occurring in 0.5 to 1 per 1,000 live births worldwide (Persson *et al*., 2005; Perenc et. al., 2022; Jakiela et. al., 2023), and causing injury in many regions of the central nervous system (Eskandari *et al*., 2004; Robert *et al*., 2021). The structural changes in the brain that accompany this disorder have been well described; some of which are stretching of the ependymal layer with loss of cilia, thinning of the corpus callosum, extracellular edema, damage to axons in the periventricular white matter, the proliferation of astrocytes, alteration of biochemical composition and synaptic potentials in hippocampal neurons, and reduced cortical thickness have been observed to correlate with the degree of hydrocephalus (Del Bigio *et al*., 2003; Olopade *et al*., 2012). The pathophysiology of hydrocephalus-induced brain damage is multifactorial and associated with the destruction of periventricular axons through a combination of mechanical injury (stretch), accumulation of waste products in the CSF, impaired blood flow, and calcium-mediated axo-skeletal damage (Del Bigio, 2004). Damage in the periventricular white matter may be associated with behavioral deficits (Del Bigio *et al*., 2003) while the pathogenesis of brain damage has been elucidated by pathological studies of human brains using experimental animal models which have been developed in a range of species either by using a variety of methods to induce hydrocephalus or through genetic mutations (Di Curzio, 2018).

Cisternal injection of sterile kaolin causes chemical arachnoiditis resulting in obstructive hydrocephalus from impairment of the flow of cerebrospinal fluid in the basal cisterns (Del Bigio, 2001; Warf, 2005). It is a well-accepted agent for inducing hydrocephalus in infant and adult animals (mice, rats, rabbits, hamsters, cats, and dogs) via injections into the subarachnoid space (Ii, 2019). Neuroinflammatory responses to ventricular enlargement have been reported in rodent models of hydrocephalus induced by sterile kaolin injection at birth (Del Bigio, 2010; Deren *et al*., 2010; Khan *et al*., 2006), juvenile (Olopade *et al*., 2012) and adult ages (Ge *et al*., 2021; Lopes *et al*., 2009; Xu *et al*., 2012).

There seems to be a paucity of literature on the mortality rate of adult mice models of hydrocephalus using sterile kaolin as well as sterile kaolin concentrations below 250mg/ml. We

**Author for Correspondence:* Tel: +2348022912220 E-mail: *temitayoshokunbi@yahoo.com*

therefore investigated the mortality rate, hydrocephalic rate, and morphological changes of pyramidal neurons of layer V of sensorimotor cortex and hippocampal regions of adult mice using different concentrations of sterile kaolin.

MATERIALS AND METHODS

Adult albino male mice (7-8weeks old) were obtained from the colony established at Central Animal House of the Faculty of Basic Medical Sciences of the University of Ibadan and housed in the faculty's Central Animal House were divided into two groups: Experimental group (n=135) and control group (n=15). All procedures on animal handling conformed to the acceptable guidelines on the ethical use of animals in research and approval for the study was obtained from the University of Ibadan Animal Care and Use Research Ethics Committee (UI-ACUREC/027-0421/21). The mice in the experimental group were further sub-divided into 5 groups (n=27 each) and initially anesthetized with intraperitoneal injection of ketamine/xylazine combination at 90/10 mg/kg and intra-cisternally injected with 0.02 mL of 5, 100, 150, 200 and 250 mg/mL of sterile kaolin respectively while the control mice received sham injection but nothing was introduced into the cisterna magna. The mice were monitored for about 1 hour in which technical mortality rates of the mice were recorded while those that survived were returned to their cages. The mice were allowed free access to water and solid pellet feed ad libitum. Biweekly body weight measurements were recorded among the groups and the mice were monitored for 4 weeks during which the development of hydrocephalus which is characterized by an enlarged or dome-shaped head, hopping gait, and general dull appearance (Olopade *et al.*, 2012) was assessed.

Animal Sacrifice and Dissection: Mice were aenesthetized and intra-cardial perfusion with 10% neutral buffered formalin was performed. Their brains were dissected and further fixed in the same solution for 48-72 hours before further processing. Brains were then sectioned at the level of the optic chiasm and ventricular diameter was measured with a digital vernier caliper (Remscheid Germany: 823-160) with a 5-digit LCD display and indication tolerance of 0.01mm.

Histology: To demonstrate Nissl body and cell count in layer V of the sensorimotor cortex and hippocampal layers, the fixed brain samples were dehydrated in increasing concentrations of ethanol (70-100%). After which they were cleared in two changes of xylene and then infiltrated at 60°c for four hours. They were embedded in paraffin wax and cooled overnight in a refrigerator at 4°c and sectioned at a thickness of 5 microns. Sections were deparaffinized in 2 or 3 changes of xylene at 10 minutes each, hydrated in 100% alcohol for 2-5 minutes, and 95% alcohol for 3 minutes. Rinsed in tap water and then distilled water. Stained in 0.1% of Cresyl violet solution, warmed up in a 37°-50°C oven, rinsed quickly in distilled water, differentiated in 95% ethyl alcohol for 2-30 minutes dehydrated in 100% alcohol, cleared in xylene, mounted and checked microscopically for best results. Well-stained sections were selected and photographed using a Leica light microscope (Leica, Germany) Average neuronal count (viable neurons) and pyknotic index were obtained by counting four serial coronal sections of four mice at X40 magnification using ImageJ software (Image J vl. 53e). The pyknotic index was calculated as (Taveira *et al* 2013):

$$\text{Pyknotic Index} = \frac{\text{pyknotic neurons}}{\text{total neurons}} \text{ X } 100$$

Immunohistochemistry for NeuN: Brain sections were also immunohistochemically stained for NeuN and the immunoreactivity test performed to assess the neuronal integrity. The selected sections were treated with 0.3% hydrogen peroxide (H2O2) in phosphate-buffered saline (PBS) for 30 min and 10% normal goat serum in 0.05 MPBS for 30 min, and diluted mouse anti-NeuN overnight at 4 °C. Thereafter, the tissues were exposed to biotinylated horse anti-mouse IgG. They were visualized by staining with 3,3′-diaminobenzidine tetrahydrochloride in 0.1 M Tris–HCl buffer (pH 7.2) and mounted on gelatin-coated slides. After dehydration, the sections were mounted with Canada balsam (Kanto, Tokyo, Japan). In order to establish the specificity of the immune staining, a negative control test was carried out with pre-immune serum instead of primary antibody. The negative control resulted in the absence of immunoreactivity in all structures.

Statistical and data analysis: Data from mortality rates, ventricular diameter, and neuronal counts were expressed as mean ±SEM and group comparison calculated using analysis of variance (ANOVA) followed by a Bonferroni post hoc test using Graph Pad prism 8.4.3.686 for Windows Software (San Diego, CA, USA). A probability value of $p<0.05$ was considered to be statistically significant. Results were presented as tables, histograms, and photomicrographs.

RESULTS

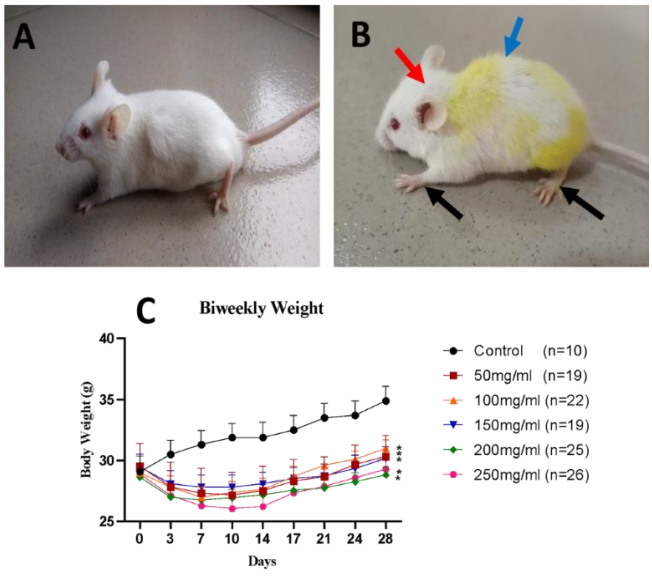

Figure 1:
Representative photographs of control (A) and hydrocephalic (B) mice. Note the dome-shaped head (red arrow), hunched back (blue arrow), scruffy fur and flat placement of the limbs (black arrow) in the hydrocephalic mouse compared to the control mouse. (C) line graph showing the mean biweekly body weight of control and hydrocephalic mice (*$p < 0.05$).

Physical observations: The hydrocephalic mice developed enlarged, dome-shaped heads that were seen from the third day of sterile kaolin injection. They also had hunched back, unsteady gait, scruffy fur and exhibited a reduction in weight,

activity, and food and water intake compared to control mice (Figure 1A and B).

Body weight: The control mice gained body weight from the beginning of the study till the end while hydrocephalic mice lost body weight within the first week post-induction of hydrocephalus. However, the body weight of the hydrocephalic mice began to stabilize till the end of second week before gaining weight till the end of the study but not as much as the controls which never lost body weight (Figure 1C).

Gross examination of the brain: Gross examination of the brains sectioned coronally at the level of the optic chiasm revealed ventricular enlargement of the hydrocephalic mice which was evident with expansion of the lateral ventricles compared to the control group (Figure 2).

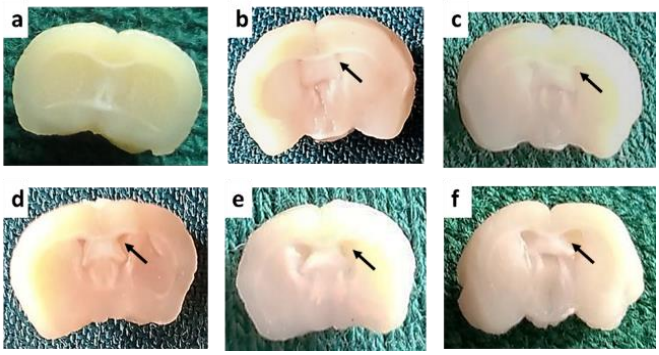

Figure 2:
Photographs of fixed brain samples of (A) control and (B, C, D, E, F) 50mg/ml, 100mg/ml, 150mg/ml, 200mg/ml, 250mg/ml of kaolin induced hydrocephalic mice respectively. The lateral ventricles of the experimental groups are enlarged compared to controls (black arrows).

Mortality rate: During induction, some animals died within a few minutes to less than 24 hours after induction due to possible brainstem puncturing, anesthetic reaction or reflex action and this was considered as technical death while the mice that survived kaolin induction but did not survive till the end of the study were considered among the mortality rate. Among the mice induced with 50mg/ml of sterile kaolin, 29.63% had technical death while the mortality rate was 21.05%. Out of the mice induced with 100mg/ml of sterile kaolin, 18.52% had technical death while the mortality rate was 22.73%. Among the adult mice induced with 150mg/ml of sterile kaolin, 29.63% of mice had technical death while the mortality rate was 26.32%. Among the mice induced with 200mg/ml and 250mg/ml of sterile kaolin, 7.41% and 3.70% had technical death while the mortality rate was 28.00% and 30.77% respectively. The mortality rate of mice induced with 250mg/ml of kaolin concentration was significantly higher than mice induced with 50mg/ml and 100mg/ml of sterile kaolin (Figure 3A). All the mice in the control group survived till the end of the study.

Frequency of hydrocephalus: In the 50 mg/mL group, 40.0% developed hydrocephalus, 58.8% developed hydrocephalus in the 100mg/ml group, 78.6% developed hydrocephalus in the 150mg/ml group, 88.9% developed hydrocephalus in the 200mg/ml group, and 94.4% developed hydrocephalus in the 250mg/ml group. Hence, the frequency of hydrocephalus was dose-dependent, being directly proportional to the dose administered, and significantly higher than the controls which did not develop hydrocephalus (Figure 3B).

Ventricular diameter: The ventricular diameter in hydrocephalic mice was higher than the control mice, which was only significant in the mice induced with 150mg/ml, 200mg/ml, and 250mg/ml of kaolin concentrations (Figure 3C).

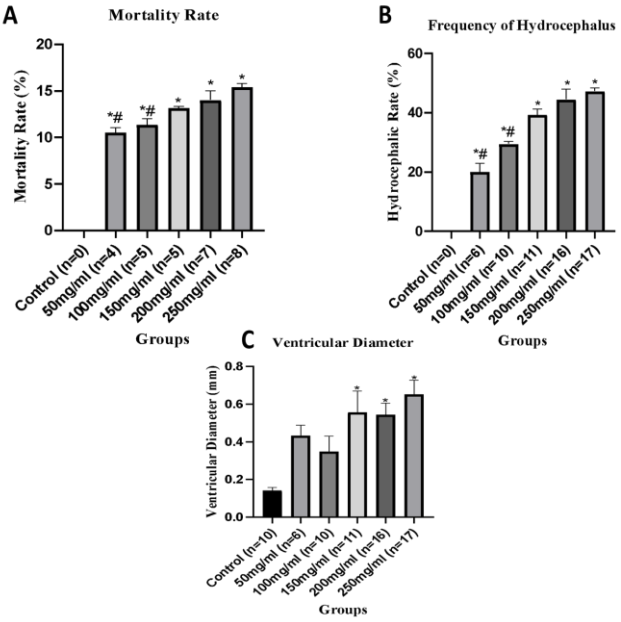

Figure 3:
Bar chart of (A) mortality rate ($p<0.0001$), (B) frequency of hydrocephalus ($p<0.0001$), and (C) ventricular diameter ($p=0.0002$) of control and hydrocephalic adult mice

Histological analysis of Layer V of sensorimotor cortex: Cresyl violet-stained neuropil of the sensorimotor cortices of the control mice revealed round and viable pyramidal neurons with few dark shrunken neurons termed pyknotic neurons. In the neuropil of sensorimotor cortices of hydrocephalic mice, there were few viable neurons and many abnormal, dark, and shrunken neurons with vacuoles mostly in the cortices of mice induced with 250 mg/mL of kaolin concentration (Figure 4A-F).

Neuronal count: Quantitative analysis of the neurons showed that the pyknotic pyramidal neurons in the internal pyramidal layer of sensorimotor cortices of hydrocephalic mice were significantly more numerous than those of the controls. Furthermore, the pyknotic neurons of mice induced with 250 mg/mL kaolin were significantly more numerous ($p<0.0001$) than those induced with 50mg/mL, 100mg/mL, and 150 mg/mL of kaolin concentrations (Figure 4G).

Histological analysis of hippocampal regions: Cresyl violet-stained hippocampal regions (CA1, CA3, and dentate gyrus) showed organized cytoarchitecture of pyramidal neurons in control and hydrocephalic mice with dilatation of lateral ventricles of hydrocephalic mice (Figure 5).

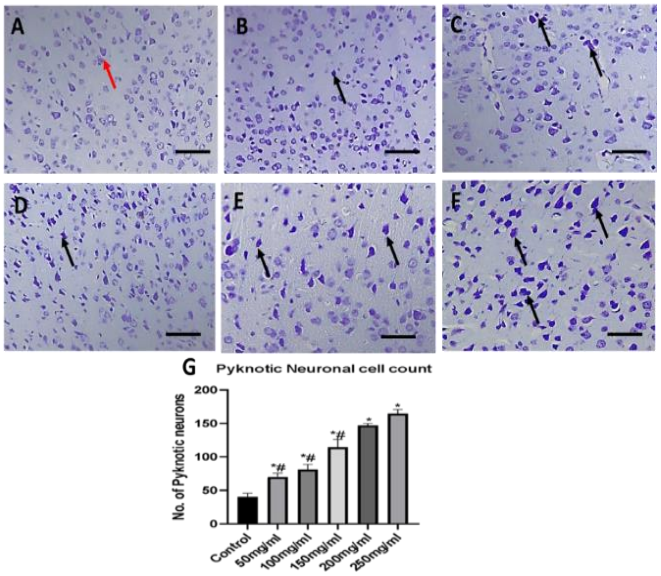

Figure 4:
Photomicrograph of Cresyl violet-stained internal pyramidal layer of the sensorimotor cortices of control (A) and hydrocephalic mice (B, C, D, E, F; 50mg/ml, 100mg/ml, 150mg/ml, 200mg/ml, 250mg/ml of kaolin respectively). There are pyknotic neurons (black arrows) in the neuropil of sensorimotor cortices of the hydrocephalic groups compared to the normal neurons (red arrow) in the control. G: Bar chart of pyknotic neuronal cell count of the internal pyramidal layer of sensorimotor cortices of control and hydrocephalic mice (Scale bar: 50μm).

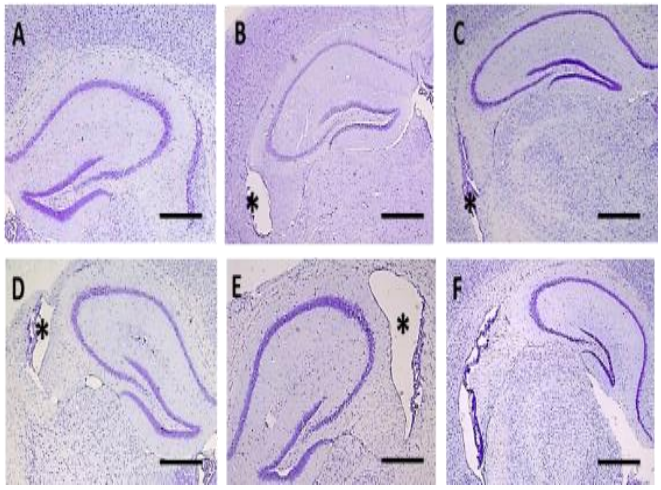

Figure 5:
Photomicrograph of cresyl violet stained hippocampus of (A) control and (B, C, D, E, F: 50mg/ml, 100mg/ml, 150mg/ml, 200mg/ml, 250mg/ml of kaolin induced hydrocephalic mice respectively). The lateral ventricles of hydrocephalic mice were enlarged (asterisks) compared to the control (Scale bar: 100μm).

In the hippocampal regions of the control mice, there were numerous round, large, and viable pyramidal neurons with distinct nuclei and few dark and shrunken neurons while the hydrocephalic mice had few viable neurons with many abnormal, dark and compressed neurons surrounded by vacuoles especially in the CA3 and dentate gyrus of mice induced with 250mg/ml of kaolin concentration (Figure 6A-F; 7A-F; 8A-F).

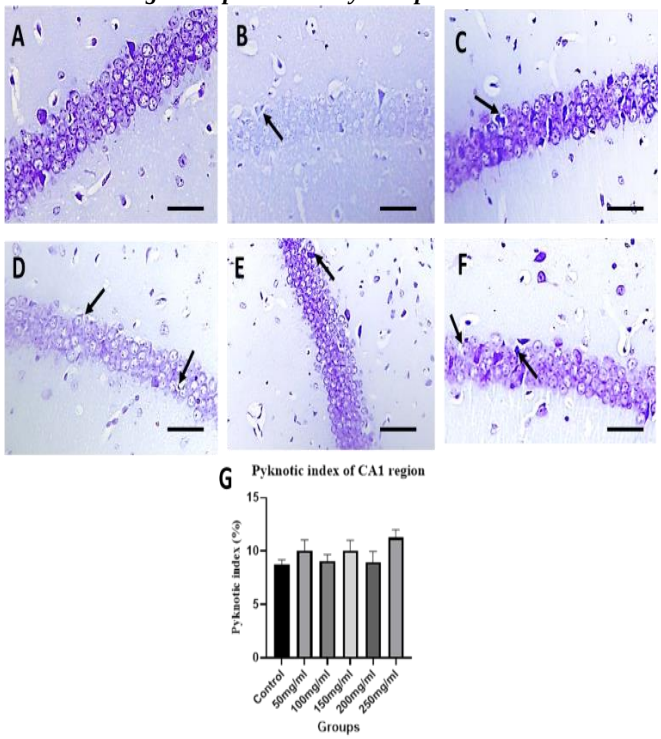

Figure 6:
Photomicrograph of cresyl violet stained CA1 of control (A) and (B, C, D, E, F: 50mg/ml, 100mg/ml, 150mg/ml, 200mg/ml, 250mg/ml of kaolin induced hydrocephalic) mice showing pyknotic neurons (black arrows) in CA1 region of the hippocampus. G: Bar chart of showing pyknotic indices of control and hydrocephalic mice. (Scale bar: 50μm).

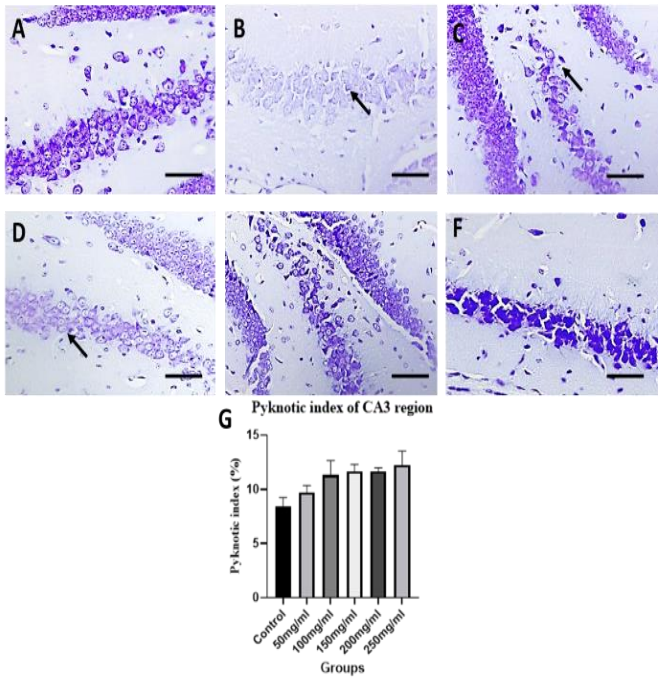

Figure 7:
Photomicrograph of cresyl violet stained CA3 of control (A) and (B, C, D, E, F) 50mg/ml, 100mg/ml, 150mg/ml, 200mg/ml, 250mg/ml of kaolin induced hydrocephalic mice showing pyknotic neurons (black arrows). (G) Bar chart of pyknotic index of all the groups (Scale bar: 50μm).

Pyknotic Index of the neurons of the hippocampal regions:
Pyknotic index of the CA1 and CA3 regions presented no statistical difference between the hydrocephalic mice

(p=0.3121; p=0.0852) when compared with the control mice, though there was an increase in the hydrocephalic mice (Figure 6G-8G). Comparison of the pyknotic index of mice induced with 250mg/ml of kaolin concentration and other concentrations in the CA1 and CA3 regions also revealed no significant difference (Figure 6G & 7G). However, the pyknotic index of the neurons of the dentate gyrus of the 250mg/ml kaolin concentration group was significantly higher (p=0.0059) than the mice induced with 50mg/ml and 100mg/ml (Figure 8G).

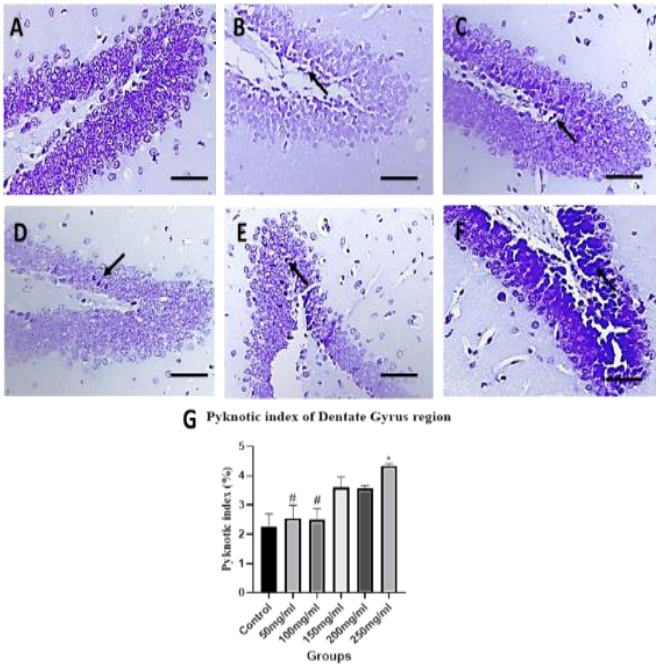

Figure 8:
Cresyl violet-stained dentate gyrus of control (A); B, C, D, E, F: 50, 100, 150, 200 and 250 mg/mL of kaolin induced hydrocephalic mice. Pyknotic neurons (black arrows) abound in the neuropil of the different concentrations of kaolin induced hydrocephalic mice; (G) Pyknotic index of the dentate gyrus neurons among all the groups (*p < 0.05; #p=0.0059; scale bar: 50μm).

NeuN+ immunoreactivity of the neurons of the sensorimotor cortices: NeuN immunostained sensorimotor cortices revealed an increased staining intensity in control mice compared to the hydrocephalic mice. There were more viable neurons in the control group compared to the hydrocephalic groups which had a lot of pyknotic neurons (Figure 9A-F). Quantification of the NeuN+ immunoreactivity of the internal pyramidal layer of the sensorimotor cortices of the control mice was significantly higher than the experimental groups (150mg/ml, 200mg/ml, 250mg/ml). NeuN+ immunoreactivity of the 150mg/ml, 200mg/ml and 250mg/ml groups were significantly lower compared to the control group (*p < 0.05) while the 250mg/ml group was significantly lower than the 50mg/ml and 100mg/ml groups (#p=0.9814) Moreover, the NeuN+ immunoreactivity of the mice induced with 250mg/ml kaolin concentration was significantly lower when compared with the mice induced with 50mg/ml and 100mg/ml of kaolin.

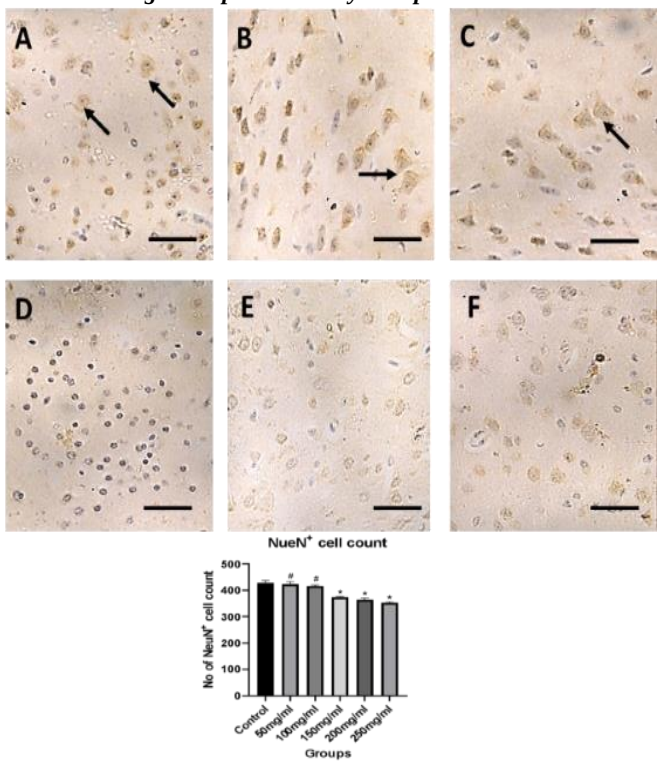

Figure 9:
NeuN immunostained internal pyramidal layer of the sensorimotor cortices of (A) control and (B, C, D, E, F) 50, 100, 150, 200 and 250 mg/mL of kaolin-induced hydrocephalic mice. Note the abundance of NeuN+ neurons (black arrows) in A,B,C. (G) Bar chart of NeuN+ immunoreactivity of the internal pyramidal layer of sensorimotor cortices of the different experimental groups (Scale bar: 20μm).

DISCUSSION

Experimental hydrocephalus induced by intracisternal kaolin injection is still the most commonly used method (Del Bigio, 2001; 2010; Di Curzio, 2018) and an effective method for producing hydrocephalus in rodents, although results are variable and somewhat unpredictable (Khan *et al*., 2006; Di Curzio, 2018). Even when using the same dose and concentration, the dispersion of kaolin suspension in the subarachnoid space varies. This may account for the relatively unpredictable rate and magnitude of ventricular dilatation that transpires. However, it is worthy of note that the kaolin model of hydrocephalus is a simple, inexpensive, and consistent way of inducing hydrocephalus in experimental animals (Del Bigio, 1993; Khan *et al*., 2006; Duru *et al*., 2019; Hamid *et al*., 2023).

We assessed the biweekly body weight of the adult mice and we were able to demonstrate that hydrocephalus was associated with reduced body weight with varying concentrations of kaolin. Even though the mice gained weight as the experiment progressed, this gain did not measure up to those of the control mice. Body weight loss is a common feature in hydrocephalic animals (Hatta *et al*., 2006; Johnston *et al*., 2013; Di Curzio *et al*., 2014; Zhang *et al*., 2015; Olopade *et al*., 2016; Liu *et al*., 2021).

The comparison of the mortality rates of adult mice induced with the same volume of 0.02ml but different concentrations of sterile kaolin suspension (50mg/ml, 100mg/ml, 150mg/ml, 200mg/ml, 250 mg/mL) into the cisterna magna was established, and we found out that some adult mice died 24hrs after induction, this mortality seen might be due to brainstem

puncturing, anesthetic reaction, respiratory failure or reflex action and can all be termed "technical death" (Olopade *et al*., 2019; Khan *et al*., 2006; López *et al*., 2009; Zhang *et al*., 2015). In addition, some mice also died before the end of the study. This might be due to neurological deficits such as spinal cord damage and subdural hemorrhage (Olopade *et al*., 2012). The mortality rate among the experimental groups was 21.05%, 22.73%, 26.32%, 28%, and 30.77% respectively. The values obtained for the mortality rates indicated a progressive increase as the concentration of kaolin increased. These findings agree with previous studies (Lollis *et al*., 2009; López *et al*., 2009) which reported that a reduction in kaolin dosage reduced the mortality rate. Zhang *et al*., (2015) reported a low mortality rate of adult rats induced with 30mg/ml of sterile kaolin. In their study, different concentrations of kaolin suspension (10mg/ml, 30mg/ml, 50mg/ml, 100mg/ml, 200mg/ml, 250mg/ml, 400mg/ml, and 500mg/ml) were used in a small-sample experimental design to determine the experimental concentration of kaolin. They observed high mortality rates among animals induced with high concentrations of kaolin suspensions.

Comparing the frequency of hydrocephalus of these adult mice was established and we found out that the frequency of hydrocephalus among the mice induced with the different concentrations was 40 %, 58.82%, 78.57%, 88.89%, and 94.4% respectively. It therefore means that the frequency of hydrocephalus of adult mice induced with 250mg/ml of kaolin had the highest number of positive outcomes compared to the lower concentrations. A high hydrocephalic rate of 90% was reported by Olopade *et al*., (2012), where 250mg/ml of sterile kaolin was used in inducing experimental hydrocephalus in juvenile rats. Taveira *et al*., (2013) reported a hydrocephalic rate of 81% using 200mg/ml of kaolin to induce hydrocephalus in neonatal rats. Hence, this agrees with our studies which show that the higher the concentration of kaolin suspension, the higher the frequency of hydrocephalus.

The hallmark of hydrocephalus is enlarged ventricles. The degree of ventricular enlargement of adult mice induced with 50mg/ml, 100mg/ml, 150mg/ml, 200mg/ml, and 250mg/ml concentrations of sterile kaolin were demonstrated, and we discovered that the lateral ventricles of all hydrocephalic mice were enlarged compared to controls. Similar findings were reported by Femi-Akinlosotu *et al*., 2021; López *et al*., 2009, Rammling *et al*., 2008; Eskandar *et al*., 2004, Bloch *et al*., 2006 and Klinge *et al*., 2003. However, the ventricles of the hydrocephalic mice were only mildly enlarged possibly because they were adults. López *et al*., (2009) reported minimal enlargement of the lateral ventricles of kaolin-induced adult mice compared to juvenile mice which were severely enlarged, while Klinge *et al*., (2006) had a similar experience in rats and Traveira *et al*., (2013) reported that hydrocephalus developed more readily in the youngest rats. However, there was no correlation between the concentration of kaolin suspension and the degree of ventricular enlargement (López *et al*., 2009).

The effect of hydrocephalus on the sensorimotor cortex of the adult hydrocephalic mice was examined through the cytoarchitectural pattern and morphology of the pyramidal neurons of the internal pyramidal layer of the sensorimotor cortex and it was observed that the cresyl violet stained sections of the sensorimotor cortex of the hydrocephalic mice revealed no visible disorganization in the cytoarchitectural pattern. This might be due to the fact that the mice all had mild ventriculomegaly. Olopade *et al*., (2019) found out that disorganization of the cytoarchitectural pattern of kaolin-induced rats corresponds with the degree of ventriculomegaly. Del Bigio (2001; 2004; 2010) concluded that the deleterious effect of hydrocephalus on the brain depends on the magnitude of ventriculomegaly, while Catalão *et al*., (2013) reported that the cytoarchitecture of the cerebral cortex in hydrocephalic rats showed signs of destruction, especially in the animals with severe ventricular dilation. These stained sections also revealed numerous large and active internal pyramidal neurons in the neuropil of the control mice group compared to mice induced with different concentrations of kaolin where there were numerous pyknotic neurons. This shows that hydrocephalus affects the morphology of the internal pyramidal neurons of the sensorimotor cortex. Chen *et al*., (2017) reported that the shapes of the cortical and hippocampal pyramidal neurons were altered following 250mg/ml kaolin induction in juvenile rats. Liu *et al*., (2021) confirmed that the number of surviving neurons reduced in the cortex and hippocampus of adult mice induced with 100mg/ml of kaolin compared to controls.

The pyknotic neuronal density of the adult mice was assessed and it was observed that a significant increase in pyknotic neuronal density is related to the increase in severity of ventriculomegaly which might be due to parenchyma compression by the enlarging ventricles. There is a paucity of knowledge on the pyknotic neuronal density of kaolin-induced hydrocephalic animals. However, López *et al*., (2009) injected a first batch of adult and juvenile mice with 250mg but 0.025 and 0.01 ml of kaolin respectively, and subsequently injected the second batch of animals with 200mg but 0.01 and 0.05ml of kaolin respectively, and the third batch of animals with 100 mg but 0.01 and 0.05ml of kaolin respectively same as the fourth batch and found out that higher concentration of kaolin suspensions was more viscous, spread less easily through the CSF pathways and were associated with more complications. In addition, Hassan and Gless, (1990) reported that most pyknotic cells appeared at the early stage of hydrocephalus. On the other hand, Jones *et al*. (1991) reported that the total cell number decreased throughout the cerebral cortex during hydrocephalus and pyramidal neuron density decreased in very late stages of ventriculomegaly in 30-day-old HTx rats with congenital hydrocephalus.

Examining the effect of hydrocephalus on the cytoarchitectural pattern and morphology of pyramidal neurons of CA1, CA3, and dentate gyrus (DG) of the hippocampus, we observed that the cytoarchitectural pattern in these regions in the mice induced with varying concentrations exhibited clumsy and compressed pyramidal neurons compared to controls which were more distinct. We had earlier reported mild disarray of the pyramidal cells layering, and abnormal clumping of chromatin in the hippocampus of kaolin-induced hydrocephalic adult mice (Shokunbi *et al*., 2020) while Taveira et. al., (2012) had reported only mild cytoarchitectural pattern disruption in kaolin induced neonatal rats even with severe ventriculomegaly. Furthermore, the neuropil of the CA1, CA3, and DG hippocampal regions of the control mice showed numerous large and active pyramidal neurons while the neuropil of the hydrocephalic mice revealed darker and shrunken neurons, these observations correspond with Burak et. al., (2011), Taveira *et al*., (2012) and Femi-Akinlosotu et. al., (2021).

The pyknotic index of CA1, CA3, and dentate gyrus regions of these adult mice were established and we ascertained that there was no significant difference between the pyknotic index of CA1 and CA3 regions of adult mice induced with varying

concentrations of kaolin and controls while the pyknotic index of adult mice induced with 250mg/ml of sterile kaolin was more than that of mice induced with other concentrations. Shokunbi *et al*., (2020) also reported a significant increase of the pyknotic index of CA1 in mice examined one week after hydrocephalus development compared to controls but not in two and three weeks of hydrocephalus development. Meanwhile, the pyknotic index of the CA3 region did not differ between experimental and control groups at all the time points after induction. López *et al*., (2009) also reported that there was no overt neuronal loss in the hippocampus of hydrocephalic mice although some neurons were pyknotic.

There was no appreciable difference in the morphology of the neurons of the dentate gyrus of hydrocephalic mice induced with 50mg/ml, 100mg/ml, 150mg/ml, and 200mg/ml concentrations of kaolin compared with the controls. However, the pyknotic index of the dentate gyrus of controls was significantly lower than the pyknotic index of the dentate gyrus of mice induced with 250mg/ml concentration of kaolin. In addition, the pyknotic index of the dentate gyrus of mice induced with 250mg/ml was significantly higher than those induced with 50mg/ml and 100mg/ml kaolin concentrations. There is limited work done on the dentate gyrus of the hippocampus in adult animals.

NeuN staining was used to assess the neuronal damage of the sensorimotor cortex of the adult mice and it further confirmed that hydrocephalus reduced the number of surviving neurons in the sensorimotor cortex compared to age-matched controls. The NeuN immunoreactivity in the controls revealed a positive reaction with an increased staining intensity compared to the hydrocephalic mice. The positive immunoreactivity of NeuN reduced in the internal pyramidal neurons of the sensorimotor cortex of kaolin-induced mice compared to controls which was consistence with the reduction in the number of internal pyramidal neurons in cresyl stained sections of hydrocephalic mice compared to controls indicating significant neuronal damage compared to the controls, which agrees with the work of Samanci *et al*., (2019), who had demonstrated significantly less NeuN-positive cells in the cortex of hydrocephalic animals reflecting altered neuronal integrity.

The use of sterile kaolin suspension in experimental hydrocephalus research is not new, however, the effect of the different concentrations of this agent needs to be well documented. This study has been able to document the effects of different concentrations of sterile kaolin suspension on the sensorimotor cortex and the hippocampus of adult mice. Our study was limited to mild ventriculomegaly which might have accounted for the little or no difference between the controls and the hydrocephalic mice. We recommend that 150mg/ml concentration of kaolin would be a better option for a long-term study that aims at getting a reasonable number of dilated ventricles because mice induced with this concentration of kaolin had low mortality rate, frequency of hydrocephalus, and ventricular dilatation compared to other concentrations. However, for a short-term study that aims at having a high frequency of hydrocephalus, 250mg/ml of kaolin concentration would be the best option, because mice induced with this concentration of kaolin had the highest frequency of hydrocephalus. Furthermore, if the objective of the study is to investigate the pathological effect of hydrocephalus on the internal pyramidal neurons of the sensorimotor cortex as well as the pyramidal neurons of hippocampal regions, 250mg/ml of sterile kaolin would be the best option, because the internal pyramidal neurons of sensorimotor cortex as well as the pyramidal neurons of hippocampal regions of mice induced with this concentration presented the highest pyknotic cells. However, further studies on the severity of hydrocephalus in adult mice using different concentrations of sterile kaolin suspension would be appreciated. The use of more detailed and confirmatory staining techniques to ascertain the effects of the hydrocephalic insults on the cytoarchitecture of the brain is also advised.

Acknowledgment:
The authors appreciate the assistance of Mr. Oludare Osuntade, Mrs. Elizabeth Ogunsola, and Mrs. Folashade Adunola during the histology processing of the brain tissues.

REFERENCES

Azzam, A. M. N., Yehia, A., Abd El-Bary, T. H., & El-Sharkawy, A. M. E. (2023). Pathophysiology and Classification of hydrocephalus. *Tobacco Regulatory Science (TRS)*, 3381-3403.

Bloch, O., K I. Auguste, G.T. Manley, and A.S. Verkman. 2006. Accelerated progression of kaolin-induced hydrocephalus in aquaporin-4-deficient mice. *J. Cereb Blood flow Metab*. 26:1527–1537.

Bothwell, S. W., Janigro, D., & Patabendige, A. (2019). Cerebrospinal fluid dynamics and intracranial pressure elevation in neurological diseases. *Fluids and Barriers of the CNS*, 16(1), 1-18.

Cabuk, B., E. Volkan, U.B. Suheyla, S. Aydin, and C. Savas. 2011. Neuroprotective effect of memantine on hippocampal neurons in infantile rat hydrocephalus. *Turk Neurosurgery* 21:352-358.

Catalão, C.H., A.L. Correa, and L.d.S. Lopes. 2013. Camellia sinensis neuroprotective role in experimentally induced hydrocephalus in Wistar rats. *Childs Nerv Syst*. 30:591-597.

Chen, L., Y. Wang, J. Chen, and G. Tseng. 2017. Hydrocephalus compacted cortex and hippocampus and altered their output neurons in association with spatial learning and memory deficits in rats. *Brain Pathology* 27:419–436.

Del Bigio, M.R. 1993. Neuropathological changes caused by hydrocephalus. *Acta Neuropathol*. 85:573–585.

Del Bigio, M. R. 2001. Future Directions for Therapy of Childhood Hydrocephalus: A view from the Laboratory. *Pediatr Neurosurg*. 34:172–181.

Del Bigio, M.R., M. Wilson, and T. Enno. 2003. Chronic hydrocephalus in rats and humans: white matter loss and behavior changes. *Ann Neurol*. 53:337–346.

Del Bigio, M.R. 2004. Cellular Damage and Prevention in Childhood Hydrocephalus. *Brain Pathol*. 14:317-324.

Del Bigio, M.R. 2010. Neuropathology and structural changes in hyrdrocephalus. *Dev Disabil Res Rev*. 16:16-22.

Deren, K., M. Packer, O. Abdullah, E. Hsu, and Ii, J.P.M. (2010). Reactive astrocytosis, microgliosis and inflammation in rats with neonatal hydrocephalus. *Exp Neurol*. 226:110–119.

Di Curzio, D.L., E. Turner-Brannen, and M.R. Del Bigio. 2014. Oral antioxidant therapy for juvenile rats with kaolin-induced hydrocephalus. *Fluids and Barriers of the CNS*. 11:1-23.

Di Curzio, D.L. 2018. Animal Models of Hydrocephalus. *J. Modern Neurosurg*. 8:57-71.

Eskandari, R., J. P. Mcallister, J. M. Miller-monfils, and Y. Ding. 2004. Effects of hydrocephalus and ventriculoperitoneal shunt therapy on afferent and efferent

connections in the feline sensorimotor cortex. *J Neurosurg*. 101:196-210.

Duru, S., Oria, M., Arevalo, S., Rodo, C., Correa, L., Vuletin, F., . . . Peiro, J. L. (2019). Comparative study of intracisternal kaolin injection techniques to induce congenital hydrocephalus in fetal lamb. *Child's Nervous System*, 35, 843-849.

Femi-akinlosotu, O.M., M.T., Shokunbi, T. Naicker, and G. Elston. 2019. Dendritic and Synaptic Degeneration in Pyramidal Neurons of the Sensorimotor Cortex in Neonatal Mice With Kaolin-Induced Hydrocephalus. *Front Neuroanat*. 13:1–10.

Femi-akinlosotu, O.M., M.T. Shokunbi, F.E. Olopade and P. Igbong. 2021. Deficits of Learning and Spatial Memory are Associated with Increased Pyknosis of Pyramidal Neurons of the Hippocampus of Adult Rats with Chronic Hydrocephalus. *West Afr J Med*. 38:1042-1049.

Ge, Y., Q. Lai, W. Wang, and X. Xu. 2021. Delayed transient obstructive hydrocephalus after cerebral aneurysm rupture. A case report. Medicine (Baltimore). 100:19-22.

Hale, P.M., J.P. McAllister II, S.D. Katz, L.C. Wright, T.J. Lovely, D.W. Miller, B.J. Wolfson, A.G. Salotto, and D.V. Shroff. 1992. Improvement of cortical morphology in infantile hydrocephalic animals after ventriculoperitoneal shunt placement. *Neurosurgery*. 31:1085-89.

Hamid, R., Gomes, V., Huda, N., Khan, A., Chowdhury, M., & Azam, I. (2023). Role of Ommaya Reservoir in Pediatric Hydrocephalus: Experience in Bangladesh Medical College Hospital from 2019-2021. *Mymensingh Med J*, 32(2).

Hasan, M., and Gless. 1990. Ultrastructural features of the human frontal cortex neurons of maturing and hydrocephalic cerebrum. *Arch Ital Anat Embriol*. 95:17-26.

Hatta J., T. Hatta, K. Moritake and H. Otani. 2006 Heavy water inhibiting the expression of
transforming growth factor–β1 and the development of kaolin-induced hydrocephalus in mice. *J Neurosurg*, 104:251-258.

Ii, J.P.M. 2019. Experimental Hydrocephalus: Models and stduy methods. Giuseppe Cinallli M.

Memet Ozek Christian Sainte-Rose Editors. Pediatric Hydrocephalus Second Edition. 1:37-51.

Jakiela, J., Billavara, M., Kaliaperumal, C., & Kumar, A. H. (2023). An overview of hydrocephalus and shunts used in the clinical management of hydrocephalus. *J Neuro and Spine*, 1(3), 83-93.

Johnston, M.G., M.R. Del Bigio, J.M. Drake, D. Armstrong, D.L. Di Curzio, and J. Bertrand. 2013. Pre- and post-shunting observations in adult sheep with kaolin-induced hydrocephalus. *Fluids Barriers CNS*. 10:24.

Jones H.C., R.M. Bucknall, and N.G. Harris. 1991. The cerebral cortex in congenital hydrocephalus in the H-Tx rat: A quantitative light microscopy study. *Acta Neuropathol*. 82:217-224

Khan, O.H., T.L. Enno, and M.R. Del Bigio. 2006. Brain damage in neonatal rats following kaolin induction of hydrocephalus. *Exp Neurol*. 200:311–320.

Klinge P.M, A. Samii, A. Muhlendyck, *et al*., 2003. Cerebral hypoperfusion and delayed hippocampal response after induction of adult kaolin hydrocephalus. Stroke. *J of the American Heart Association.* 34:193-199.

Klinge P.M, A. Samii, S. Niescken T. Brinker and G.D. Silverberg. 2006. Brain amyloid accumulates in aged rats with kaolin-induced hydrocephalus. *Neuroreport*. 17:657-660.

Liu, C., Y. Chen, W. Cui, Y. Cao, L. Zhao, H. Wang, X. Liu, S. Fan, K. Huang, A. Tong, and L. Zhou. 2021. Inhibition of neuronal necroptosis mediated by RIP1/RIP3/ MLKL provides neuroprotective effects on kaolin-induced hydrocephalus in mice. Cell Proliferation. *Int J Mol Sci*. 23:735.

Lollis, S., J. Hoopes, S. Kane, K. Paulsen, J. Weaver, and D. Robberts. 2009. Low-dose kaolin-
induced feline hydrocephalus and feline ventriculostomy. *J Neurosurg Pediatr.* 4:383-388.

Lopes, S., I. Slobodian, and M.R. Del Bigio 2009. Characterization of juvenile and young adult mice following induction of hydrocephalus with kaolin. *Experimental Neurology*. 219:187-196.

McMullen, A.B., G.S. Baldwan, and K.D. McCarthy. 2012. Morphological and behavioural changes in the pathogenesis of a novel mouse model of communicating hydrocephalus. *J Neurosci Res*. 89:142-152.

Olopade, F.E., M.T. Shokunbi, and A-L. Sire´n. 2012. The relationship between ventricular dilatation, neuropathological and neurobehavioural changes in hydrocephalic rats. *Fluids and Barriers of the CNS*. 9:19.

Olopade, F.E., and M.T. Shokunbi. 2016. Neurobehavioral Deficits in Progressive Experimental Hydrocephalus in Neonatal Rats. *Niger. J Physiol. Sci*. 31:105-113.

Olopade, F.E., M.T. Shokunbi. I.A. Azeez, A. Andrioli, I. Scambi, and M. Bentivoglio. 2019. Neuroinflammatory response in chronic hydrocephalus in juvenile rats. *J Neuroscience*. 419:14-22.

Perenc, L., Guzik, A., Podgórska-Bednarz, J., & Drużbicki, M. (2022). Somatic development disorders in children and adolescents affected by syndromes and diseases associated with neurodysfunction and hydrocephalus treated/untreated surgically. *International Journal of Environmental Research and Public Health*, 19(9), 5712.

Persson, E., G. Hagberg, and P. Uvebrant. 2005. Hydrocephalus prevalence and outcome in a population-based cohort of children born in 1989 – 1998. *Actaa Paediart*. 94:726-732.

Robert, S. M., Reeves, B. C., Marlier, A., Duy, P. Q., DeSpenza, T., Kundishora, A., . . . Alper, S. L. (2021). Inflammatory hydrocephalus. *Child's Nervous System*, 37(11), 3341-3353.

Rammling, M., M. Madan, L. Paul, B. Behnam, and J.V. Pattisapu. 2008. Evidence for reduced lymphatic CSF absorption in the H-Tx rat hydrocephalus model. *BioMed Central Cerebrospinal Fluid Research.* 5:15.

Samanci, M.Y., S.E. Celik, Z.U. Coskun, and D. Ozcan. 2019. Radiological, biomechanical and histopathological characteristics of rat brain in Kaolin-induced hydrocephalus. *Romanian Neurosurgery*. 10:498-507.

Shokunbi, M.T. F.E. Olopade, O.M. Femi-Akinlosotu, and E.O. Ajiboye. 2020. Pyramidal cell morphology and cell death in the hippocampus of adult mice with experimentally induced hydrocephalus. *Niger J Paediatr*. 47:298-304.

Taveira K.V, K.T. Carraro C.H. Catalão and L.da.S. Lopes. 2013. Morphological and morphometric analysis of the hippocampus in Wistar rats with experimental hydrocephalus. *Pediatr Neurosurg*. 48:163-167.

Warf, B. 2005. Hydrocephalus in Uganda: The predominance of infectious origin and primary management with endoscopic third ventriculostomy. *J Neurosurg*. 102:1-15.

Xu, H., G. Tan, S. Zhang, H. Zhu, F. Liu, C. Huang, F. Zhang, and& Z. Wang. 2012. Minocycline reduces reactive gliosis in the rat model of hydrocephalus. *BMC Neurosci*. 13:148.

Zhang S., Z. Wang, H. Xu F. Zhang C. Huang D. Chen, D., Bao, F. Liu and S. Shen. 2015. Hydrocephalus induced via

intraventricular kaolin injection in adult rats. *Folia Neuropathol*. 53:60-68